

Laser-like X-ray Sources Based on Optical Reflection from Relativistic Electron Mirror

H.-C. Wu^{1,*}, J. Meyer-ter-Vehn², J. Fernández¹, and B.M. Hegelich^{1,3}

¹*Los Alamos National Laboratory, Los Alamos, New Mexico 87545, USA*

²*Max-Planck-Institut für Quantenoptik, D-85748 Garching, Germany*

³*Department für Physik, Ludwig-Maximilians-Universität München, D-85748 Garching, Germany*

(Dated: February 4, 2022)

A novel scheme is proposed to generate uniform relativistic electron layers for coherent Thomson backscattering. A few-cycle laser pulse is used to produce the electron layer from an ultra-thin solid foil. The key element of the new scheme is an additional foil that reflects the drive laser pulse, but lets the electrons pass almost unperturbed. It is shown by analytic theory and by 2D-PIC simulation that the electrons, after interacting with both drive and reflected laser pulse, form a very uniform flyer freely cruising with high relativistic γ -factor exactly in drive laser direction (no transverse momentum). It backscatters probe light with a full Doppler shift factor of $4\gamma^2$. The reflectivity and its decay due to layer expansion is discussed.

PACS numbers: 41.75.Jv, 52.59.Ye, 52.38.Ph

High-quality X-ray sources are requested in many fields of science. Presently, large free-electron lasers (FEL) [1] represent powerful coherent VUV and X-ray sources, which open a new era of intense VUV or X-ray interaction with matter and provide unprecedented opportunities for research in condensed matter physics, high-energy-density physics [2] and single biomolecular imaging [3]. High laser harmonics from gas targets [4] and relativistic laser plasma interaction [5] are also very useful and promising coherent X-ray sources. Such harmonic sources typically produce trains of sharp spikes separated by the time period of the driving laser pulse.

Bright and coherent X-ray sources can also be obtained by coherent Thomson scattering (CTS) from dense electron layers flying with relativistic factor $\gamma_x = 1/\sqrt{1 - \beta_x^2}$. Here $\beta_x = v_x/c$ is the velocity of the plane flyer in normal direction. Counter-propagating probe light is then mirrored and frequency-upshifted by the relativistic Doppler factor, which is $(1 + \beta_x)/(1 - \beta_x) \approx 4\gamma_x^2$ for $\gamma_x \gg 1$ [6]. In this paper we refer to these electron layers as relativistic electron mirrors (REM) or simply flyers. One way to produce them is to drive cold non-linear plasma waves to the point of wave breaking. Their density profile then develops diverging spikes that may move with high γ_x -factors [7]. Recent experiments have demonstrated $\gamma_x \approx 5$ by identifying the mirrored light [8]. This method is limited by the phase velocity of the plasma wave requiring low plasma density for high γ_x -factors of the wave. Higher densities can be achieved by accelerating thin solid foils. Corresponding simulations were reported recently [9], driving a 250 nm thick foil with a laser intensity of about 10^{23} W/cm^2 . Only small γ_x values are obtained in this case, because the complete foil including ions is accelerated.

In this letter, a different regime is considered requiring much lower laser intensities and foils thin enough

for the laser pulse to push out all electrons from the foil. In this case, only electrons are accelerated and can gain high γ values, while the heavy ions are left behind unmoved. For this to happen, the normalized laser field $a_0 = eE_{L,0}/mc\omega_L$ has to be much larger than the normalized field arising from charge separation, $E_{x,0} = (n_e/n_c)k_L d$. Here $\omega_L = ck_L$ is the circular frequency of the driving laser pulse, n_e is the electron density and d the thickness of the foil initially, while $n_c = \epsilon_0 m_e \omega_L^2 / e^2$ is the critical density. This regime has been described by Kulagin in a number of papers (see e.g. [10]), and coherent Thomson scattering (CTS) from the emerging relativistic electron layers has been studied in Refs. [11, 12]. Some typical results are shown in Fig. 1. The scheme requires extremely thin foils of a few nanometer and laser pulses with a very high contrast ratio in order not to destroy the target before the main pulse arrives. These foils are much thinner than the skin depth and are therefore transparent, even though the electron density is overcritical. The leading edge of the laser pulse ionizes the foil and takes the electrons along as a thin sheath (see Fig. 1(a) and Fig. 2). Their motion is well described in a single-electron picture [13, 14]; transverse and longitudinal momenta follow approximately the local laser vector potential $a(x, t)$ according to $p_\perp = a$, $p_x = \gamma - 1 = a^2/2$, where γ is now the full relativistic factor.

There are two severe drawbacks, when using these flyers as REMs for reflecting probe light. First, the flyer $\gamma(t)$ depends on time such that the reflected pulse is chirped and has a broad spectrum. Secondly, the mirror γ_x is much smaller than the full γ for $\gamma \gg 1$ (see Fig. 1(b)). In fact, we find for the Doppler shift

$$4\gamma_x^2 = 4\gamma^2/(1 + p_\perp^2) \approx 2\gamma. \quad (1)$$

Apparently, the transverse momentum p_\perp , inherent to electron motion in transverse light waves, degrades the upshift. This is true even though the angle of electron motion relative to the laser direction, $\tan \theta = p_\perp/p_x = 2/a$, tends to vanish for large a .

*hcwu@lanl.gov

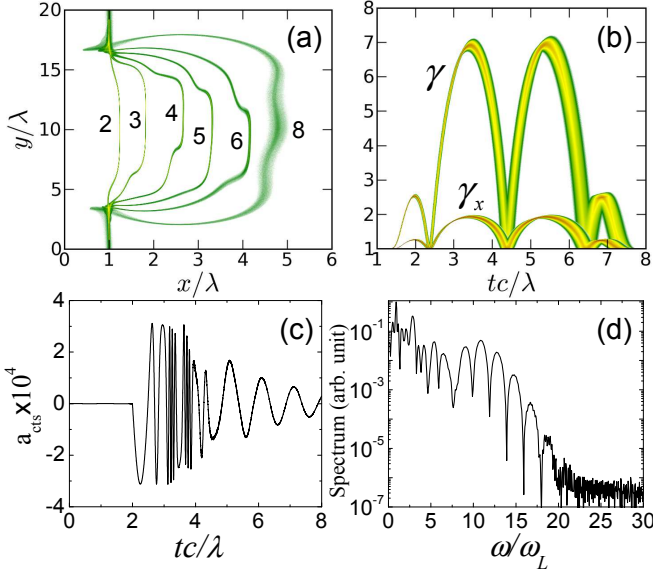


FIG. 1: (color). Laser-driven electron layer blown out from a thin foil at $x/\lambda = 1$ by a drive laser pulse incident from the left in $(+x)$ -direction and reflected light from a probe pulse incident from the right in $(-x)$ -direction. (a) Simulated electron density in (x, y) plane given at different times in units of c/λ ; (b) temporal evolution of γ_x and γ ; (c) probe light reflected from the electron layer as seen by an observer at $x/\lambda = 6$; (d) corresponding spectrum.

The major result reported in this Letter is a method to overcome these two drawbacks and to describe a practical way to generate flyers that have fixed γ values and $\gamma_x \approx \gamma$. Accordingly, they can produce optical pulses that are Doppler-shifted by the full factor $4\gamma^2$ and have a narrow spectrum. They are only limited by decreasing reflectivity due to decay of the flyer. The way to suppress the transverse momentum is to let the electrons interact with a counter-propagating laser pulse. Here the central new observation is that reflection of the drive pulse from a perfect mirror provides the ideal interaction pulse. The corresponding configuration is sketched in Fig. 2. Due to relativistic kinematics, the reflected pulse changes the energy γ of the flyer electrons only marginally, but eliminates their transverse momentum p_\perp completely. While the electrons gain energy $(\Delta\gamma)^+ \propto a^2$ when co-moving with the driving pulse for a long time, the interaction time with the reflected counter-propagating pulse is quite short, and, accordingly, the energy loss is only of order unity, $(\Delta\gamma)^- \propto 1$; this we have discussed in more detail in Ref. [11].

Here we restrict ourselves to show explicitly only the elimination of p_\perp . Let us denote electric and magnetic field of the plane drive pulse by $E^+ = B^+ = f(t - x)$ (fields normalized to $m\omega_L/e$). Reflection from a perfect mirror at $x = x_R$, taking due account of a phase-shift π , produces the reflected pulse $E^- = -B^- = -f(t + x - 2x_R)$. The electron transverse momentum obeys $dp_\perp/dt = -(E^+ + E^-) + \beta_x(B^+ + B^-)$. It can

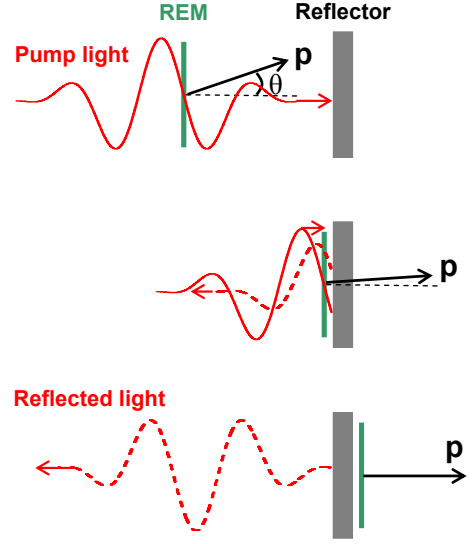


FIG. 2: (color). Schematic drawing of electron layer (green) surfing on laser drive pulse and reflector foil (grey). Electron momentum is tilted by angle θ relative to laser pulse axis. Middle part: The drive pulse is reflected by the reflector foil and interacts a second time with the electron layer. Lower part: The fully reflected drive pulse propagates to the left, while the electron layer has passed the reflector foil and is cruising to the right at constant velocity and free of transverse momentum.

be obtained as the sum $p_\perp = p_\perp^+ + p_\perp^-$ of the momenta resulting from the interaction with drive and reflected pulse separately. These are described by

$$\frac{dp_\perp^+}{dt} = -(1 - \beta_x)f(t - x), \quad (2a)$$

$$\frac{dp_\perp^-}{dt} = (1 + \beta_x)f(t + x - 2x_R). \quad (2b)$$

Using new coordinates $\tau^+ = t - x(t)$ with $d\tau^+/dt = 1 - \beta_x$ in Eq. (2a) and $\tau^- = t + x(t) - 2x_R$ with $d\tau^-/dt = 1 + \beta_x$ in Eq. (2b), one obtains the equations $dp_\perp^+/d\tau^+ = -f(\tau^+)$ and $dp_\perp^-/d\tau^- = f(\tau^-)$, which are independent of the particular form of the electron trajectories $x(t)$ and $\beta_x = dx/dt$. Here we integrate the first one from $\tau^+ = 0$, when the drive pulse first touches the electron, toward $\tau^+ = \tau_R$, when the electron hits the reflector. We also integrate the second one from $\tau^- = t_2 + x(t_2) - 2x_R = 0$, when the reflected wave front reaches the electron at time $t_2 = 2x_R - x(t_2)$ and location $x(t_2)$, toward $\tau^- = \tau_R$. We find that the two momenta obtained from interaction with drive pulse and reflected pulse exactly cancel each other such that the electron emerging from behind the reflector foil has $p_\perp = 0$ and therefore $\gamma_x = \gamma$. Apparently, this result holds for each individual electron of the flyer independent of its initial distance from the reflector and the laser pulse shape $f(\tau)$. It is also independent of the charge separation field which eventually causes longitudinal dispersion of the mirror. The deeper reason for the cancellation of p_\perp lies in the fact that, due to planar

symmetry, the invariance $p_{\perp} = a$ still holds for the combined fields $a = a^+ + a^-$ of forward-going and reflected pulse, and therefore $p_{\perp} \rightarrow 0$ since $a \rightarrow 0$ when passing the reflector [15].

We have checked these results by two-dimensional particle-in-cell (2D-PIC) simulations [16]. Figure 1 exhibits electron expulsion from a thin foil and CTS of probe light from the emerging electron flyer for the case without reflector. Here the simulation box has a size of $10\lambda \times 20\lambda$ in xy plane, and a space resolution of 1000 cells/ λ and 800 cells/ λ in x - and y - direction, respectively. The pump laser pulse has a profile $a_0 \sin^2(t/T)$ with pulse duration $T = 3\lambda/c$. The carrier-envelope-phase of the laser is set to zero, so that the electric field maximum is at the pulse center. The transverse profile is chosen as a super-Gaussian $\exp(-r^4/R^4)$ with waist $R = 5\lambda$. We take $a_0 = 3.5$, corresponding to an intensity of $I = 2.6 \times 10^{19}$ W/cm² for $\lambda = 800$ nm.

Few-cycle pulses of this strength are presently becoming available [17]. The laser pulse is linearly p -polarized along the y -direction and injected into the simulation box from the left boundary at $t = 0$. For this exploratory simulation, the initial ultrathin foil is chosen with density $n_e/n_c = 1$, thickness $L/\lambda = 0.001$, and is located at $x_0 = 1\lambda$. The initial plasma temperature is 10eV, and the ions are taken as immobile. The total number of macro-particles is about 5×10^7 .

The electron density evolution is shown in Fig. 1(a). An electron layer is driven out of the foil (immobile ions at $x/\lambda = 1$ not shown), and one may notice some transverse electron motion in polarization (y) direction superimposed on the drift in laser (x) direction. Due to the transverse shaking, the effective area available for CTS is limited to the central zone between $9 < y/\lambda < 11$. The temporal evolution of γ and γ_x is shown in Fig. 1(b) for electrons located between $9.5 < y/\lambda < 10.5$. The energy spread of the electron layer increases with time and eventually leads to gradual longitudinal expansion. One also notices the conspicuous difference between γ and γ_x . The maximum values $\gamma_{\max} \approx 7.0$ and $\gamma_{x,\max} \approx 1.8$ agree with the single-electron prediction $\gamma_x \approx \sqrt{\gamma/2}$ (see Eq.(1)). The evolution of $\gamma(t)$ follows approximately the laser vector potential according to the single-electron expression $\gamma(t) = 1 + a(x(t), t)^2/2$. After $t = 8\lambda/c$, the laser pulse has overtaken the electrons, which then return to rest in agreement with the Lawson-Woodward theorem [18].

Signatures of probe light incident from the right side and backscattered from the relativistic electron layer are also shown in Fig. 1. In the simulation, the probe pulse is taken as a plane wave, $a_p(x, t) = a_{p0} \cos(k_L x + \omega_L t)$, and s -polarized (in z -direction) to distinguish it from the drive pulse. A relatively small amplitude $a_{p0} = 0.1$ is chosen to make sure that the scattering is linear and that the flyer shape is not strongly perturbed. The reflected light is recorded by a fictitious observer located at $(x, y) = (6\lambda, 10\lambda)$. The temporal shape and spectrum of the reflected signal are shown in Fig. 1(c) and Fig. 1(d), respectively. By adjusting the time delay, we make

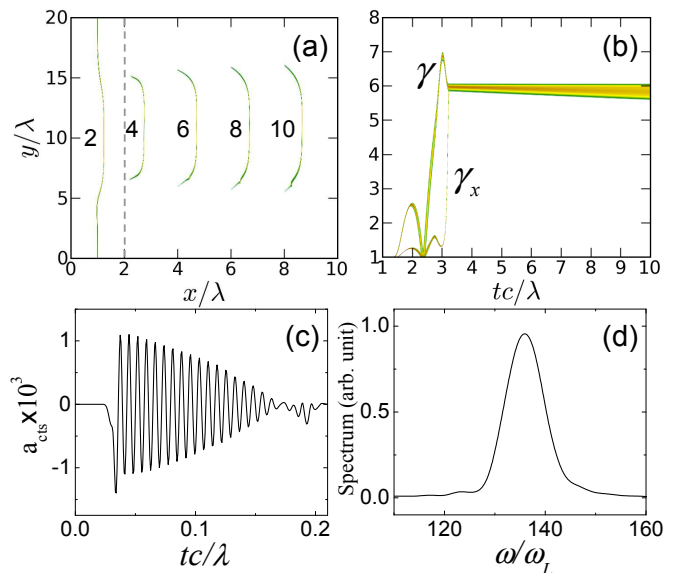


FIG. 3: (color). Same as Fig. 1, but now including the 24 nm thick reflector foil. (a) A very uniform electron layer is emerging from the reflector foil (dashed line at $x_R/\lambda = 2$); (b) at about $t \approx 3c/\lambda$, when the electron flyer passes the reflector foil, γ_x approaches γ , indicating elimination of transverse electron momentum; the electron energy is given by nearly constant $\gamma = \gamma_x \approx 5.9$, and the energy spread increases slightly with time indicating layer expansion; (c) the reflected probe light appears as a regular, Doppler-compressed light wave that decays due to decreasing reflectivity of the expanding electron layer; (d) the spectrum shows a narrow VUV pulse Doppler-shifted by $4\gamma_x^2 \approx 139$ corresponding to a wavelength of 5.7 nm for 800 nm probe light. For more details see text.

sure that the fronts of both pump and probe pulse touch the production foil at the same time. The reflected signal therefore contains the whole information on the flyer dynamics. Since the Doppler shift $4\gamma_x(t)^2$ varies with time, a complex oscillation pattern is observed in the reflected signal, leading to the broad spectrum seen in Fig. 1(d); the cut-off appears at $\omega/\omega_L = 4\gamma_x^2 \approx 16$ in agreement with the peak values of $\gamma_x \approx 2$. The two groups of rapid oscillations represent the two γ_x peaks in Fig. 1(b) and cause the spectral beating with period $\Delta\omega/\omega_0 \approx 2$. Though interesting as a diagnostics of flyer dynamics, such CTS pulses are of little value as a light source.

These results change drastically when adding the reflector foil. The configuration is illustrated in Fig. 2. Simulation results corresponding to those in Fig. 1, but now including the reflector, are depicted in Fig. 3. They highlight the central results of this Letter. It is observed that the electrons emerge from the reflector foil (marked by the dashed line in Fig. 3(a)) as a smooth dense layer in distinct contrast to the distorted shape seen in Fig. 1. In Fig. 3(b) one sees γ_x sharply rising and almost exactly merging with γ at a value of $\gamma_x = \gamma \approx 5.9$, while γ itself drops only by $\Delta\gamma \approx 1$. This is due to the interaction with the reflected drive pulse. As predicted above on the basis of single-electron motion, interaction with the

reflected pulse fully eliminates transverse electron momentum, while reducing electron energy only marginally.

Although these sudden changes occur close to the reflector foil, it is important to understand that they are not due to any direct action of the reflector foil on the electrons, but are mediated indirectly by the reflected laser field. The reflector foil is modeled here as a fully ionized plasma slab with a density of $n_{e,R}/n_c = 400$ and a thickness of $L_R/\lambda = 0.03$. This is sufficient to fully reflect the drive pulse. A reflectivity of 99.8% is obtained in the simulation. On the other hand, the relativistic electron layer passes the thin reflector foil practically unperturbed. The relative energy loss due to Coulomb collisions is found to be negligible in the order of 10^{-5} .

It appears that a uniform relativistic electron flyer with constant γ is produced that can now act as a CTS mirror. Backscattering of probe light by this mirror has been simulated, using the same parameters as for the results of Fig. 1, but now increasing space resolution in x -direction to 1500 cells/ λ in order to resolve the CTS signal of much higher frequency and also enlarging the box length in x -direction to 15λ . The reflected signal now consists of a regular wave train strongly compressed by the moving mirror (see Fig. 3(c)) and with a spectral peak (see Fig. 3(d)), Doppler-shifted by the factor $4\gamma_x^2 = 4\gamma^2 \approx 139$ in best agreement with $\gamma = 5.9$. Here the observation point has been moved to $(x, y) = (13\lambda, 10\lambda)$ to record the full CTS signal. Although the probe light is incident continuously, the CTS signal decays due to the expansion of the flyer clearly seen in Fig. 3(c). For an incident wavelength of $\lambda = 800$ nm, the X-ray pulse has a duration of about 500 attoseconds and a central wavelength of 5.7 nm. The maximum amplitude of $a_{cts} = 1.4 \times 10^{-3}$ corresponds to the intensity of 4.2×10^{12} W/cm² and to a reflectivity of about 10^{-6} . By slightly changing the parameters, we expect that a pulses of 10^9 coherent X-ray photons are possible covering the range of the water window.

The coherent reflectivity of these electron flyers has been studied in Ref. [12]. For a flyer density distribution $n_e(x) = n_{e,0}S(x/L_c)$, given by a symmetric shape function $S(x/L_c) = S(-x/L_c)$ with characteristic length L_c , the CTS amplitude in normal direction can be obtained as

$$a_{cts} = a_{p0} \frac{n_{e,0}}{2\gamma n_c} F(\xi). \quad (3)$$

where $F(\xi)$ is the Fourier transform

$$F(\xi) = \int_{-\infty}^{\infty} S(\chi/\xi) \cos(2\chi) d\chi. \quad (4)$$

Here $\chi \equiv k'_L x'$ and $\xi \equiv k'_L L'_c$ denote the normal-

ized x coordinate and layer thickness in the rest frame of the electron flyer; in the lab frame ξ is given by $\xi = \gamma^2(1 + \beta)k_L L_c$. A similar form-factor $F(\xi)$ appears in the theory of coherent synchrotron radiation [19]. For a Gaussian profile $S(x) = \exp(-x^2/L_c^2)$, we find $F(\xi) = \sqrt{\pi}\xi \exp(-\xi^2)$. Apparently, for such a shape the reflected signal vanishes exponentially as soon as $\xi \gg 1$, i.e. when the flyer becomes thicker than the wavelength of the reflected, $L_c \gg \lambda/4\gamma^2$. For the parameters studied above, we have $n_{e,0} = 0.252n_c$, $L_c = 0.0017\lambda$ (Gaussian fitting), $\gamma = 5.96$, and obtain $a_{cts} = 1.6 \times 10^{-3}$ in reasonable agreement with the PIC result shown in Fig. 3(c). The conversion ratio of pulse energy is found from Eq. (3) as

$$\alpha = \frac{n_{e,0}^2}{4n_c^2} \frac{F(\xi)^2}{\gamma^4(1 + \beta)^2}. \quad (5)$$

In conclusion, we have described a new method to make high-quality, micro-scale, relativistic electron mirrors. Dense electron layers, driven out from nanometer-thick production foils by few-cycle laser pulses, are significantly improved by introducing an additional reflector foil that reflects the drive laser pulse, but lets the electrons pass unperturbed. As a result, very uniform relativistic electron layers are obtained, freely cruising at fixed high- γ values precisely in drive-laser direction and with zero transverse momentum. Here we have discussed coherent Thomson backscattering from these layers to generate monochromatic, coherent, soft x-ray pulses, Doppler-shifted by a factor $4\gamma^2$. The goal was to explain basic features in terms of single-electron dynamics and verifying the scheme by 2D-PIC simulation. The next step will be experimental demonstration. Though demanding, both the generation of the required high-contrast laser pulses and the fabrication of the micro-scale double foil targets should be within range in the next future. Successful demonstration would provide a new versatile tool for generating powerful laser-like X-ray pulses on a micro-scale.

Acknowledgments

The authors are grateful to Dr. Lin Yin for useful discussions and comments and Dr. Chengkun Huang for a very helpful comment. J. Meyer-ter-Vehn acknowledges support by the Munich center for Advanced Photonics (MAP) and by the Association EURATOM - Max-Planck-Institute for Plasma Physics.

- [3] R. Neutze *et al.*, Nature **406**, 752 (2000).
- [4] J. Seres *et al.*, Nature **433**, 596 (2005).
- [5] B. Dromey *et al.*, Phys. Rev. Lett. **99**, 085001 (2007).
- [6] A. Einstein, Ann. Phys. (Leipzig) **17**, 891 (1905).
- [7] S.V. Bulanov, T.Zh. Esirkepov, T. Tajima, Phys. Rev. Lett. **91**, 085001 (2003).
- [8] A.S. Pirozhkov *et al.*, Phys. Plasmas **14**, 123106 (2007).
- [9] T.Zh. Esirkepov *et al.*, Eur. Phys. J. D **55**, 457 (2009).
- [10] V.V. Kulagin *et al.*, Phys. Rev. Lett. **99**, 124801 (2007).
- [11] J. Meyer-ter-Vehn and H.-C. Wu, Eur. Phys. J. D **55**, 433 (2009).
- [12] H.-C. Wu and J. Meyer-ter-Vehn, Eur. Phys. J. D **55**, 443 (2009).
- [13] J. Meyer-ter-Vehn, A. Pukhov, Z.-M. Sheng, *Relativistic Laser Plasma Interaction, in Atoms, Solids and Plasmas in Super-Intense Laser Fields*, edited by D. Batani et al (Kluwer Academic/Plenum Publishers, 2001).
- [14] M. Wen, J. Meyer-ter-Vehn, H.-C. Wu, B. Shen, Eur. Phys. J. D **55**, 451 (2009).
- [15] Chengkun Huang, private communication (2010).
- [16] H.-C. Wu *et al.*, Phys. Rev. E **77**, 046405 (2008); *ibid*, New J. Phys. **10**, 043001 (2008).
- [17] K. Schmid, L. Veisz, *et al.*, Phys. Rev. Lett. **102**, 124801 (2009).
- [18] P.M. Woodward, J. Inst. Electr. Eng. **93**, 1554 (1947); J.D. Lawson, IEEE Trans. Nucl. Sci. **26**, 4217 (1979).
- [19] G.P. Williams *et al.*, Phys. Rev. Lett. **62**, 261 (1989).